# Two-dimensional triangular-lattice Cu(OH)Cl, belloite, as a magnetodielectric system

Xu-Guang Zheng,[1,*] Ichihiro Yamauchi,[1] Shigeto Kitajima,[2] Masayoshi Fujihala,[2] M. Maki,[1] Sanghyun Lee,[3] Masato Hagihala,[3] S. Torii,[3] T. Kamiyama,[3] and Tatsuya Kawae[4]

[1]*Department of Physics, Faculty of Science and Engineering, Saga University, Saga 840-8502, Japan*

[2]*Department of Physics, Graduate School of Science and Engineering, Saga University, Saga 840-8502, Japan*

[3]*Institute of Materials Structure Science, KEK, Tokai 319-1106, Japan*

[4]*Department of Applied Quantum Physics, Faculty of Engineering, Kyushu University, Fukuoka 819-0395, Japan*

(Received 19 June 2018; published 2 October 2018)

Quantum spins on a triangular lattice may bring out intriguing and exotic quantum ground states. Here we report a magnetodielectric system of CuOHCl wherein $S = 1/2$ $Cu^{2+}$ spins constitute a two-dimensional triangular lattice with the layers weakly coupled via Cl-H-O bonding. Despite strong magnetic interactions, as expected from the relatively high value of $\theta_{CW} = -100$ K, antiferromagnetic transition occurred at $T_N = 11$ K, followed by an uprising turn of the magnetic susceptibility below ~7 K. Neutron-diffraction experiment revealed a coplanar spin structure on the triangular lattice below the $T_N$, with each spin pointing toward the center of a triangle. Of the three spins on a triangle, two are antiparallel and the third one is angled 120° to the antiparallel spins. A concerted effect of geometric frustration in the triangular lattice and superexchange interactions through a zig-zag path via double Cu-O-Cu and double Cu-Cl-Cu bridges counted for this spin arrangement. Further investigation using dielectric constant and heat capacity measurements, as well as a microscopic probe of muon spin rotation, revealed a magnetodielectric effect and the possibility of multiferroic transition at $T^* \sim 5$ K, which is suspected to be in close relation to geometric frustration in this triangular lattice. The present paper presents a magnetodielectric system on a two-dimensional triangular lattice with chemical stoichiometry. It can also serve as a rare reference to the hotly debated quantum spin-orbital liquid compound $LiNiO_2$.

DOI: 10.1103/PhysRevMaterials.2.104401

## I. INTRODUCTION

Geometrically frustrated magnets, in which localized magnetic moments on triangular, kagome, or pyrochlore lattices interact through competing exchange interactions, have been of intense recent interest due to the diversity in the exotic ground states that they display [1–3]. The diverse experimental reports of unconventional magnetic properties, such as magnetic monopoles, quantum spin liquids, and exotic excitations, provide challenge and testing ground for theoretical models. The triangular lattice, in particular, the $S = 1/2$ system, has the simplest spin geometric configuration for frustrated magnetism that leads to intriguing and exotic quantum ground states. It is also highly evaluated because of simplicity and adaptability for theoretical modeling. Nevertheless, experimental realization of real systems has been rare.

In previous years, we identified unconventional magnetic transitions and their relation to geometric frustration in transition-metal hydroxyhalogenide series of $M_2(OH)_3X$, as well as $M(OH)X$, where $M$ represents $d$-electron magnetic ions of $Cu^{2+}$, $Ni^{2+}$, $Co^{2+}$, $Fe^{2+}$, and $Mn^{2+}$ and $X$ represents the halogen ions of $Cl^-$, $Br^-$, or $I^-$ [4]. These hydroxyl salts exist widely in nature as minerals as well as biominerals in living organisms, with the most familiar one of $Cu_2(OH)_3Cl$ on the surface of bronze statues, imparting the characteristic hue to the Statue of Liberty. Here we report magnetodielectric effect and possible multiferroic transition in synthetic triangular-lattice Cu(OH)Cl, which is known as the mineral belloite. These properties are suspected to be in close relation to the frustrated magnetism that arises from competing interactions on the triangular lattice as discussed in Sec. III.

## II. EXPERIMENTAL METHODS AND PROCEDURES

The crystal structure of Cu(OH)Cl was first reported by Iitaka *et al.*, in 1961 [5], and further refined using small single crystals by Effenberger in 1984 [6] and by Cudennec *et al.* in 2000 [7]. They used two equivalent descriptions of different axis and unit-cell choices but the two settings gave almost the same bond distances. Only in recent years was its geometrically frustrated feature revealed by us [8,9]. The pure phase of polycrystalline, as well as small single crystals, of Cu(OH)Cl [Cu(OD)Cl for neutron diffraction], colored dark green similar to that of mineral belloite, were prepared by heating mixed powders of CuO and $CuCl_2 \cdot 2H_2O$ (in a weight ratio of 1:10) in a sealed quartz glass tube at 200–270 °C for one week to one month and then thoroughly rinsed with ethanol. All Cu(OH)Cl/Cu(OD)Cl samples were insulating, reflecting its chemical stoichiometry. Synchrotron x-ray diffraction with a wavelength of 0.49985 Å on the BL02B2 beam line at the SPring-8 synchrotron, and neutron diffraction using the superhigh resolution powder diffractometer at J-PARC, Japan, were performed, respectively, to investigate the crystal and magnetic structures. In the latter, the time-of-flight data were analyzed using the Rietveld analysis software

*Corresponding author: zheng@cc.saga-u.ac.jp

 

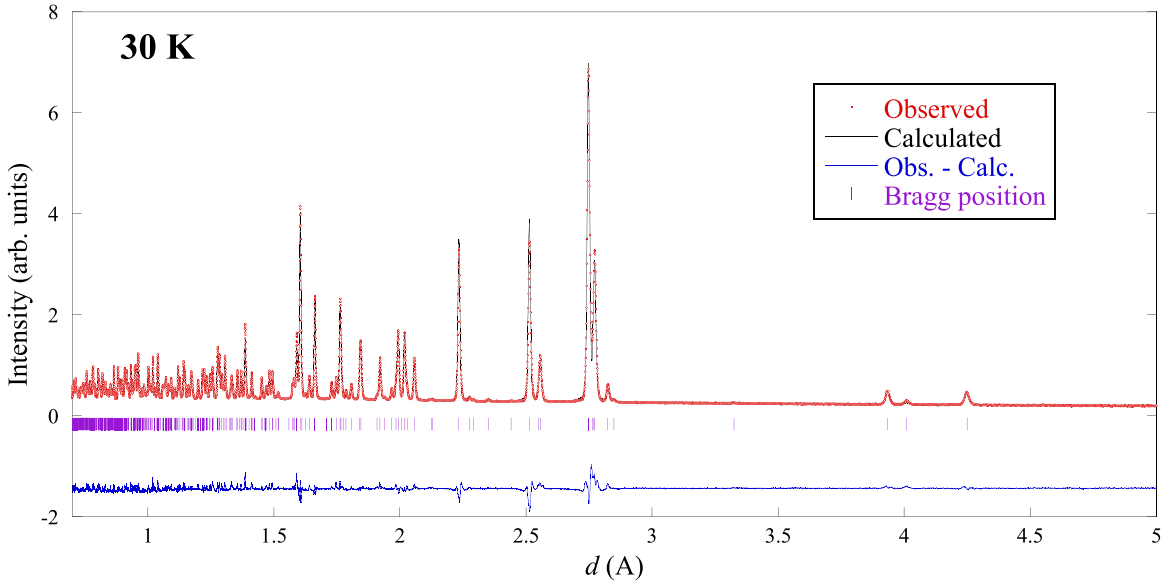


FIG. 1. Neutron powder-diffraction pattern (filled circles) for Cu(OD)Cl at 30 K and the result of Rietveld structure refinements showing the calculated (thick solid line) pattern and the difference (thin solid line on the bottom).

for J-PARC [10]. The synchrotron data were analyzed and refined using the Rietveld method with the computer program RIETAN-FP [11]. The collected neutron data were refined using the FULLPROF-suite software based on Rietveld refinement [12], assisted by the representation analysis program SARAh [13]. The dc susceptibility measurements were taken using a commercial superconducting quantum interference device magnetometer (MPMS; Quantum Design). The heat capacity was measured using an adiabatic heat-pulse method with a $^3$He cryostat using 0.5 g of the polycrystalline sample mixed with gold powder. Dielectric constants were also measured with a LCZ meter on a pellet sample of pressed powder. Muon spin rotation/relaxation ($\mu$SR) experiments were conducted on the M20 port at the muon facility of TRIUMF (Canada) using a positive surface muon beam with a conventional He gas flow cryostat. The positive muon beam, polarized to the beam direction, is stopped in the specimen and depolarized by its internal fields. The time histograms of muon decay positrons are recorded by forward ($F$) and backward ($B$) counters as a function of resident time for each $\mu^+$ within the specimen. A positron is emitted preferentially toward the muon spin direction. Therefore, asymmetry $A(t) = [F(t) - B(t)]/[F(t) + B(t)]$ of the two histograms (after correction for solid-angle effects) reflects the time evolution of muon spin polarization, as well as the time evolution and space distribution of the internal fields in the specimen.

## III. EXPERIMENTAL RESULTS AND DISCUSSION

Synchrotron x-ray diffraction at 300 K for Cu(OH)Cl and neutron diffraction data at 30 K for Cu(OD)Cl (Fig. 1) were refined to produce structural information as summarized in Tables I and II. The structure of Cu(OH)Cl/Cu(OD)Cl agreed well with those reported by Effenberger [6] and Cudennec *et al.* [7] for Cu(OH)Cl. Here we used the setting by Effenberger [6] since it is more usual to use the $c$ axis as the out-of-plane direction for layered compounds. As illustrated in Figs. 2(a) and 2(b), the $S = 1/2$ $Cu^{2+}$ ions form a fairly good triangular lattice in the $a$-$b$ plane, with a small deviation of 3.6% for the Cu-Cu distances from regular triangles, providing a suitable environment for geometric frustration. It is worth noting that the triangular lattice is largely two-dimensional both in crystal chemistry as well as in magnetic coupling. The triangular lattice layers are chemically weakly coupled via Cu-Cl-H-O-Cu bondings and magnetically weakly coupled with a long $Cu^{2+}$-$Cu^{2+}$ distance of ~6.13 Å.

TABLE I. Structure information of Cu(OD)Cl at 30 K and Cu(OH)Cl at 300 K refined from the neutron and synchrotron x-ray powder-diffraction data, respectively. All atoms are at 4*e* Wyckoff position.

| Temperature | 30 K | | | 300 K |
|---|---|---|---|---|
| Chemical formula | CuODCl | | | CuOHCl |
| Space group | $P2_1/a$ | | | $P2_1/a$ |
| $a$ (Å) | 5.54766(7) | | | 5.55605(6) |
| $b$ (Å) | 6.65507(9) | | | 6.67010(5) |
| $c$ (Å) | 6.09758(9) | | | 6.12753(7) |
| $\beta$ (deg) | 114.933(1) | | | 114.9380(9) |
| V(Å$^3$) | 204.142(5) | | | 205.9105(38) |
| $R_{wp}$ | 7.56 | | | 3.40 |
| Atom | $x$ | $y$ | $z$ | $B_{iso}$(Å$^2$) |
| | | at 30 K | | |
| Cu 4*e* | 0.2529(4) | 0.1169(4) | −0.0340(3) | 1.40(5) |
| O | 0.1471(4) | 0.3520(4) | 0.1090(5) | 0.42(4) |
| D | 0.2228(5) | 0.3390(4) | 0.2872(5) | 2.22(7) |
| Cl | 0.3216(3) | 0.4087(2) | −0.3127(2) | 0.82(3) |
| | | at 300 K | | |
| Cu 4*e* | 0.25334(12) | 0.11852(12) | −0.03237(10) | 0.798(13) |
| O | 0.14836(49) | 0.35173(52) | 0.11100(44) | 0.863(71) |
| Cl | 0.32142(21) | 0.40860(18) | −0.31091(19) | 1.036(27) |

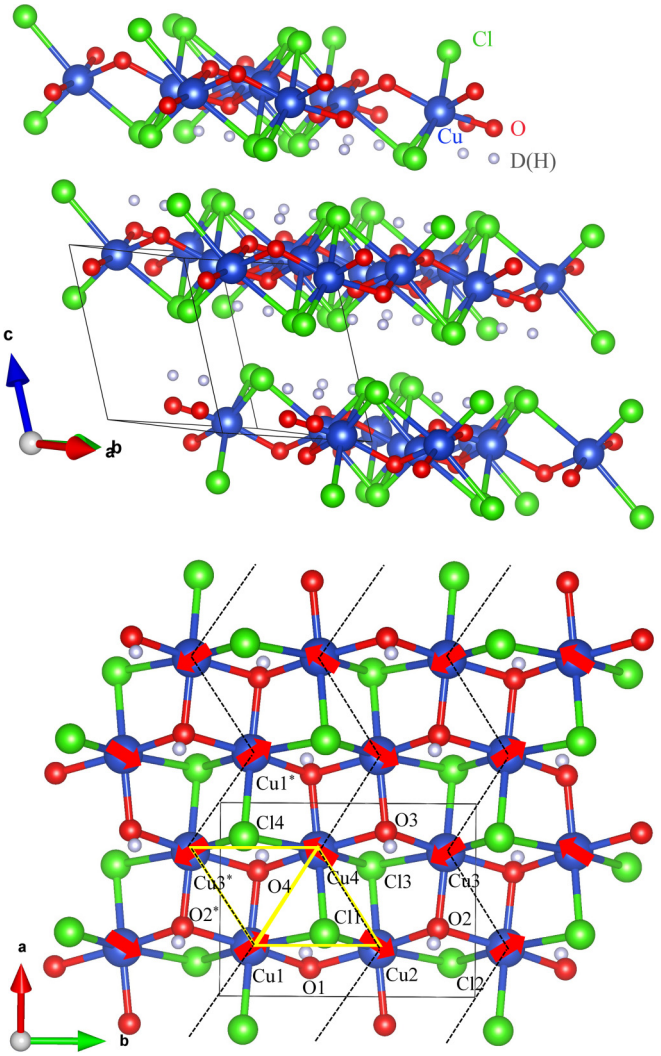


FIG. 2. (a) Crystal structure of Cu(OD)Cl. (b) Surrounding environment of $Cu^{2+}$ and spin structure in the magnetically ordered phase. The arrows show the spin directions of the $Cu^{2+}$ (blue). Each $Cu^{2+}$ (blue) is surrounded by three O (red) and three Cl (green) in a deformed octahedral coordination. The zig-zag chains show Cu-Cu couplings through superexchange interactions via Cu-O-Cu and Cu-Cl-Cu.

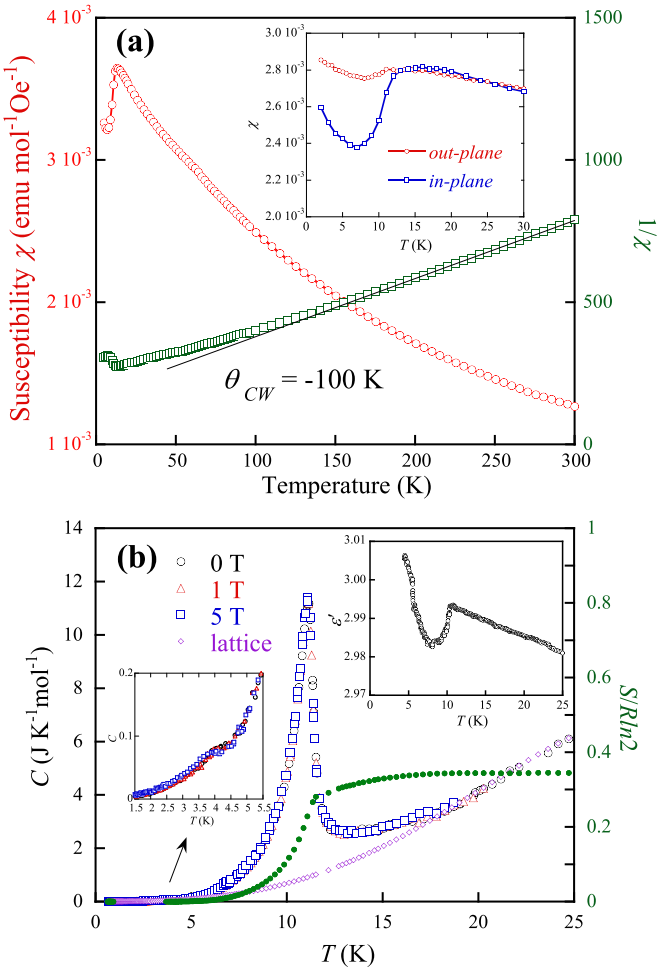


FIG. 3. (a) Temperature dependence of the susceptibilities $\chi$ (open circles, left axis) and the inverse susceptibilities $1/\chi$ (open squares, right axis) for polycrystalline Cu(OH)Cl, measured at 10 kOe. The solid line obeys the Curie-Weiss law, $\chi^{-1}(T) = (T - -\theta_w)/C$, with a Weiss temperature of $\theta_w$ of approximately $-95$ K. The inset plot shows the susceptibilities measured at 1 kOe for a small single crystal approximately along the $c$ axis and within the $a$-$b$ plane. (b) Specific heat for Cu(OH)Cl depicting a sharp transition at $T_N = 11$ K, and a microanomaly below around 5 K. The inset plot on the upper corner shows the dielectric constant changes measured at 100 kHz.

The temperature dependence of dc magnetic susceptibility for polycrystalline Cu(OH)Cl is depicted in Fig. 3(a). Antiferromagnetic transition at $T_N = 11$ K was observed, followed by an uprising turn below 7 K but still with a linear $M$-$H$ behavior. The intrinsic nature of the low-temperature upraise was verified by measurement on a single crystal as illustrated in the inset plot, as well as by the $\mu$SR results (since the amplitude of $\mu$SR signals directly reflects the volume of the individual magnetic phases and thus a microscopic amount of impurities would not affect the results). The susceptibilities at high temperatures obeyed the Curie-Weiss law, $\chi^{-1}(T) = (T-\theta_{CW})/C$, with a Curie-Weiss temperature of $\theta_{CW}$ of approximately $-100$ K, wherein the large ratio of $\theta_{CW}/T_N$ apparently indicated magnetic frustration arising from the triangular lattice. The specific heat plot in Fig. 3(b) showed a sharp transition centered at $T_N = 11$ K, and a microscopic anomaly below around $T^* \sim 5$ K, the intrinsic nature of which will be demonstrated by $\mu$SR. The magnetic entropy release for this system showed an incomplete value of 0.34 $Rln2$ in consistency with the frustration evidenced in the magnetic susceptibility. Meanwhile, the dielectric constant measured with a LCZ meter on pellet sample of pressed powders showed a rapid decrease at 11 K and recovery below ~7 K, followed by a jump at ~5 K. The successive changes in the dielectric constant at $T_N = 11$ and ~7 K apparently reflected the coupling to the magnetic states. Therefore, Cu(OH)Cl can be treated as a magnetodielectric system. The reason for the dielectric and specific-heat anomalies at $T^* \sim 5$ K will be uncovered by $\mu$SR.

The results of neutron-diffraction measurement at low temperatures for Cu(OD)Cl clearly demonstrated a long-range

TABLE II. Bond lengths and bond angles between neighboring Cu ions at 30 and 300 K for Cu(OD)Cl and Cu(OH)Cl, respectively, for an easy view of superexchange interactions.

| Temperature | 30 K | 300 K |
|---|---|---|
| Bond distance (Å) | | |
| Cu1-Cu2 = Cu3-Cu4 | 3.355(4) | 3.3602(12) |
| Cu1-Cu4 | 3.292(4) | 3.2857(11) |
| Cu2-Cu4 | 3.383(4) | 3.3942(10) |
| Cu1-Cu3* | 3.024(4) | 3.0411(10) |
| Cu1-O2* = Cu3*-O4 = Cu2-O1 | 1.959(4) | 1.983(3) |
| Cu3*-O2* = Cu1-O4 | 1.995(3) | 2.0176(19) |
| Cu1-O1 = Cu4-O4 | 1.997(4) | 2.013(3) |
| Cu1-Cl1 = Cu4-Cl4 | 2.712(3) | 2.7111(12) |
| Cu2-Cl1 = Cu4-Cl3 | 2.701(2) | 2.6949(11) |
| Cu4-Cl1 = Cu2-Cl3 | 2.2833(16) | 2.2938(8) |
| Bond angle (deg.) | | |
| Cu1-O2*-Cu3* = Cu1-O4-Cu3* | 99.82(17) | 98.94(14) |
| Cu1-O1-Cu2 = Cu4-O4-Cu3* | 116.04(15) | 114.47(12) |
| Cu1-Cl1-Cu2 = Cu4-Cl4-Cu3* | 76.61(10) | 76.86(7) |
| Cu2-Cl1-Cu4 = Cu2-Cl3-Cu4 | 85.05(10) | 85.34(8) |
| Cu1-O4-Cu4 | 111.14(17) | 109.22(14) |
| Cu1-Cl1-Cu4 | 81.97(10) | 81.60(8) |

magnetic order establishing below $T_N = 11$ K. The magnetic reflections can be indexed with the propagation vector $\boldsymbol{k} = (0, 0, 0)$. All symmetry-allowed magnetic structures derived from the representation analysis program of SARAh were examined. For the magnetic propagation vector $\boldsymbol{k} = (0, 0, 0)$ in the $P2_1/a$ crystal space group, the possible magnetic structures were represented as $\Gamma_{\text{mag}} = 3\Gamma_1(A_g) + 3\Gamma_2(A_u) + 3\Gamma_3(B_g) + 3\Gamma_4(B_u)$, where $\Gamma_i$s are the irreducible representations derived for the magnetic propagation vector $\boldsymbol{k} = (0, 0, 0)$ in this crystal space group as shown in Table III. The intensity of magnetic reflections, i.e., the difference between the intensities obtained at 5 and 30 K, and the fitting results using all symmetry-allowed magnetic structures are shown in Fig. 4. Apparently, the $\Gamma_2(A_u)$ plotted in Fig. 4(b), with fitted values of $M_x = 0.460(51)$, $M_y = 0.729(14)$, and $M_z = 0.08(14)$ resulting in a total moment of $0.85\,\mu_B$ for $Cu^{2+}$, should be the magnetic structure in the antiferromagnetic phase. As plotted in Fig. 1(b), a magnetic order for a triangular lattice was revealed: the spin directions are confined on the triangular lattice, with each spin pointing toward the center of a triangle. Of the three spins on a triangle, two are antiparallel and the third one is angled 120° to the antiparallel spins.

Inspection of the bond lengths as listed in Table II helped us to understand this spin arrangement from a viewpoint of superexchange interactions. As illustrated in Figs. 2(a) and 2(b), each $Cu^{2+}$ ion is surrounded by three O(H) and three Cl in a deformed octahedral coordination, wherein two neighboring $Cu^{2+}$ ions share a common edge. The orbitals of $Cu^{2+}$ in this much deformed octahedral crystal field should be split with the lower $t_{2g}$ orbitals fully filled. Since direct exchange comes from a direct overlap between $t_{2g}$ orbitals, superexchange interactions should dominate here. Among all $Cu^{2+}$ ions denoted in Fig. 2(b), the Cu1 and Cu3* connected via two Cu-O-Cu bridges with antiparallel spins has the shortest distance.

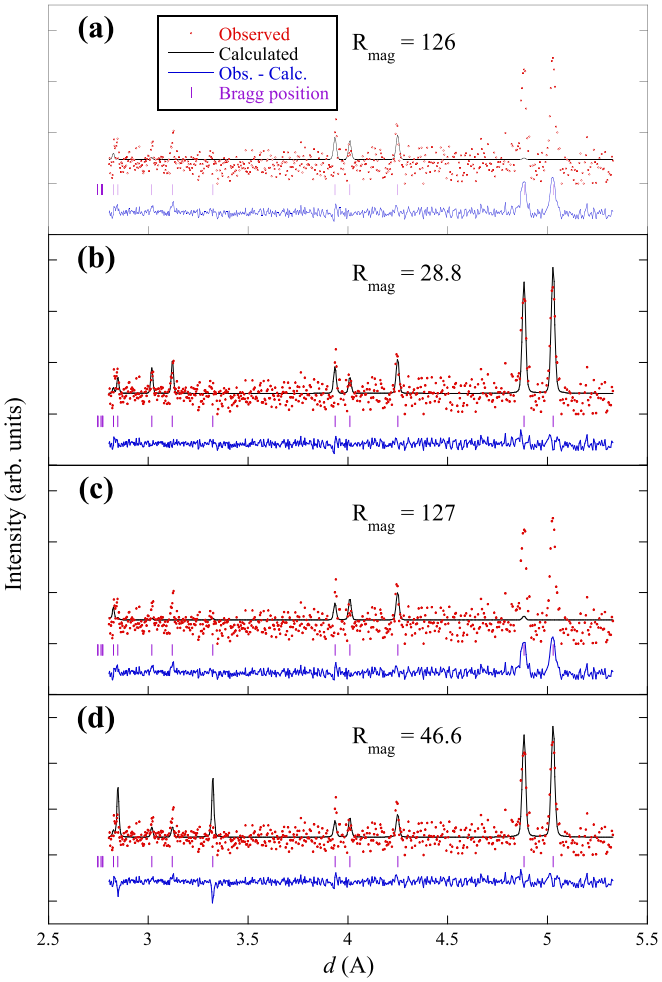


FIG. 4. The intensity of magnetic reflections fitted with possible magnetic structures of (a) $\Gamma_1$, (b) $\Gamma_2$, (c) $\Gamma_3$, and (d) $\Gamma_4$ for Cu(OD)Cl.

Apparently, strong superexchange interactions should occur via these two Cu-O-Cu bridges. Meanwhile, antiparallel spins also exist between Cu2-Cu4 bridged by two Cl, where the Cu-Cu distance is longer but with a larger orbital overlap of Cu-Cl-Cu. Therefore, superexchange interactions should exist along the zig-zag chains as denoted in Fig. 2(b). The double Cu-O-Cu and double Cu-Cl-Cu bridges showed bonding angles near 90° (~100 and 85°, respectively), wherein the classical Goodenough-Kanamori-Anderson (GKA) rules for superexchange would seemingly expect a ferromagnetic ground state. Such contradiction to the GKA rules was also seen in a hot-topic "quantum spin-orbital liquid" material of triangular lattice $LiNiO_2$ and antiferromagnetic $NaNiO_2$ [14–16]. In $LiNiO_2$ and $NaNiO_2$, the magnetic ions of $Ni^{3+}$ and nonmagnetic Li or Na stack alternatively, giving rise to a quasi-two-dimensional triangular magnetic lattice. In them, the magnetic ions of $Ni^{3+}$ are connected via two Ni-O-Ni bridges angled near 90° and its ground state was theoretically predicted to be in a low-spin configuration of $t_{2g}^6 e_g^1$ (thus direct exchange between $t_{2g}$ electrons does not occur). Reitsma *et al.* derived the spin-orbital Hamiltonian for triangular lattice $Ni^{3+}$ interacting via 90° superexchange bond and reported

TABLE III. Magnetic models $\Gamma_{\rm mag} = 3\Gamma_1(A_g) + 3\Gamma_2(A_u) + 3\Gamma_3(B_g) + 3\Gamma_4(B_u)$ obtained from representational analysis. The space group is $P2_1/a$ and the magnetic propagation vector is $k = (0\,0\,0)$.

| | Cu1 $(x, y, z)$ | Cu2 $(-x+0.5, y+0.5, -z)$ | Cu3 $(-x, -y, -z)$ | Cu4 $(x+0.5, -y+0.5, z)$ |
|---|---|---|---|---|
| $\Gamma_1(A_g)$ | $(S_x, S_y, S_z)$ | $(-S_x, S_y, -S_z)$ | $(S_x, S_y, S_z)$ | $(-S_x, S_y, -S_z)$ |
| $\Gamma_2(A_u)$ | $(S_x, S_y, S_z)$ | $(-S_x, S_y, -S_z)$ | $(-S_x, -S_y, -S_z)$ | $(S_x, -S_y, S_z)$ |
| $\Gamma_3(B_g)$ | $(S_x, S_y, S_z)$ | $(S_x, -S_y, S_z)$ | $(S_x, S_y, S_z)$ | $(S_x, -S_y, S_z)$ |
| $\Gamma_4(B_u)$ | $(S_x, S_y, S_z)$ | $(S_x, -S_y, S_z)$ | $(-S_x, -S_y, -S_z)$ | $(-S_x, S_y, -S_z)$ |

that the competing effects of local Jahn-Teller distortions and ferromagnetic superexchange can produce both ferromagnetic and antiferromagnetic interactions [17].

As a matter of fact, the present Cu(OH)Cl can serve as a good reference to the much-debated magnetic ground state in $LiNiO_2$. Ever since its synthesis in 1958 by Goodenough *et al.* [18], $LiNiO_2$ has been a subject of continuous debate. While Jahn-Teller deformed $NaNiO_2$ showed a long-range antiferromagnetic order below 20 K, the $LiNiO_2$ without Jahn-Teller deformation did not show a magnetic order down to experimentally achievable temperatures. It is believed that the octahedral crystal field acting on the nickel ions without Jahn-Teller deformation in $LiNiO_2$ brings out twofold orbital degeneracy of the $Ni^{3+}$ ($t_{2g}{}^6 e_g{}^1$) ions, leading to orbital frustration and the quantum spin-orbital liquid ground state. Theoretical interest in this system comes from the interplay between different degrees of freedom: orbital degeneracy of the $e_g$ electrons in $Ni^{3+}$ and their eventual coupling to the $S = 1/2$ spins, the effect of frustration in the triangular Ni lattice, and the elusive nature of the magnetic interactions [16].

However, there is no clear experimental evidence of what is the true orbital ground state of $LiNiO_2$. Despite tremendous publications on this material, its true ground state is still controversial and remains an open issue. The biggest problem is that $LiNiO_2$ samples are never stoichiometric because additional $Ni^{2+}$ ions always substitute $Li^+$ ions in the Li layers, leading to $[Li_{1-x}{}^{1+}Ni_x{}^{2+}][Ni_x{}^{2+}Ni_{1-x}{}^{3+}]O_2$. De Brion *et al.* [16] reported that $Li_{0.3}Na_{0.7}NiO_2$ exhibited no Jahn-Teller transition contrary to $NaNiO_2$, but it still showed a magnetic structure similar to $NaNiO_2$. Thus they concluded that $NaNiO_2$ can most probably be the spin model for the magnetic ground state of pure $LiNiO_2$.

Therefore, the spin arrangement in the two-dimensional triangular lattice system of Cu(OH)Cl can be attributed to an interplay of superexchange interactions and geometric frustration of the $S = 1/2$ spins in the triangular lattice. Apparently, the present triangular lattice Cu(OH)Cl of perfect stoichiometry, with structural deformation in the octahedral crystal field reminiscent of $NaNiO_2$, can be a rare reference to the hotly debated layered compound $(LiNa)NiO_2$. It is worth noting that the magnetic structure differs from that of $NaNiO_2$, which showed a simple A-type antiferromagnetic order with ferromagnetic intraplane coupling and antiferromagnetic interplane coupling [19,20]. This is a natural result of the weak interplane coupling in Cu(OH)Cl. In the case of $LiNiO_2$ and $NaNiO_2$, interplane coupling was sometimes considered to have a crucial effect on the contrasting magnetic behaviors in $LiNiO_2$ and $NaNiO_2$, since additional $Ni^{2+}$ ions in $LiNiO_2$ always substitute $Li^+$ ions in the interplane Li layers. The two-dimensional triangular lattice Cu(OH)Cl can be also a reference on this aspect.

The confinement of spins on the *a*-*b* plane was in good consistency with the contrastingly different changes of the susceptibilities across $T_N$ in and outside of the *a*-*b* plane, as shown in the inset plot in Fig. 3(a). Noting the absence of any change in the specific heat and the apparent stability of the magnetic structure, the susceptibility increase below 7 K was believed to be due to a microscopic spin direction adjustment.

Although direct dielectric/ferroelectric measurement on a single crystal has not been achieved yet due to the unavailability of large-enough crystals at the present stage, $\mu$SR enabled us to explore the origin of the $T^* \sim 5$ K anomaly appearing in the dielectric constant and specific heat. With a large gyromagnetic ratio $\gamma_\mu (= 2\pi \times 135.54\,\text{MHz/T})$ of the muon, where $\mu^+$ stopped nearby anions in the material, $\mu$SR is a sensitive probe to a change in the local magnetic/electric field in the solid on an atomic scale. The ZF $-$ $\mu$SR asymmetry, $A(t)$, in the paramagnetic phase, as shown in Fig. 5, showed that 79.3(7)% of the implanted muons stopped nearby $OH^-$ forming (OH)-$\mu^+$ bonding, as was often seen in materials containing hydrogen [21,22]. Their behavior was well described by a two-spin model function $G_{2s}(t) = \frac{1}{6} + \frac{1}{6}\cos(\omega t) + \frac{1}{3}\cos(\frac{1}{2}\omega t) + \frac{1}{3}\cos(\frac{3}{2}\omega t)$, where $\omega = \hbar\gamma_\mu\gamma_N/r^3$; $\gamma_\mu$ and $\gamma_N$ are the gyromagnetic ratios of $\mu^+$ and H nuclear spins, respectively; and $r = 1.64(1)$ Å is the distance between $\mu^+$ and $H^+$. The remaining 20.7% stopped

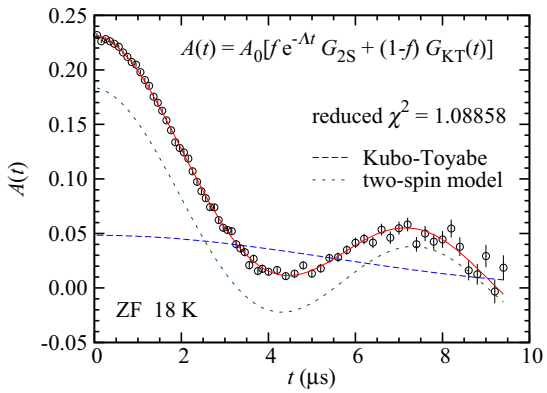


FIG. 5. The ZF $-$ $\mu$SR asymmetry at 18 K for Cu(OH)Cl, showing that the spectrum in the paramagnetic phase is well fitted by the equation including the two-spin model function $G_{2s}(t) = \frac{1}{6}[1 + \cos(\omega t) + 2\cos(\frac{1}{2}\omega t) + 2\cos(\frac{3}{2}\omega t)]$; 79.3(7)% of the implanted muons stopped nearby OH forming (OH) $-$ $\mu^+$ bonding.

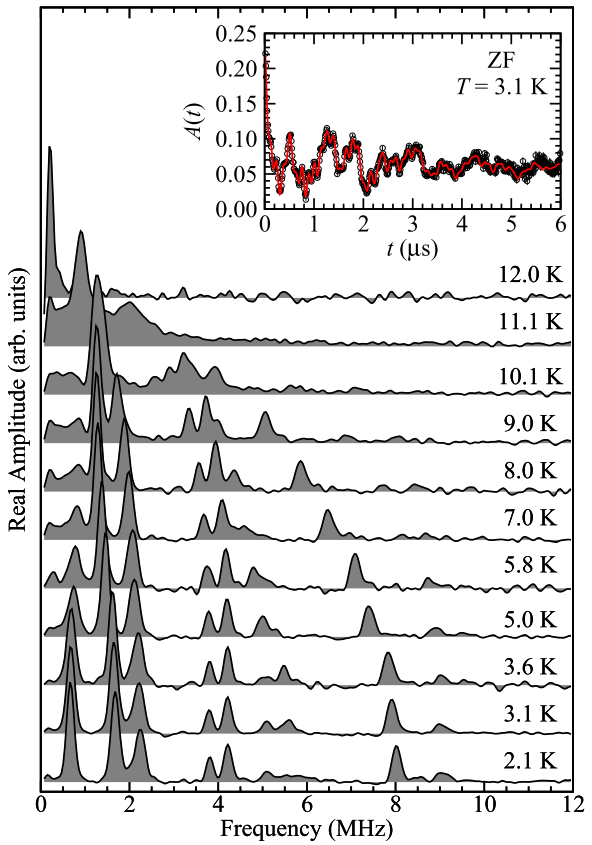


FIG. 6. Fourier transform for the zero-field $\mu$SR asymmetry spectra at typical temperatures for Cu(OH)Cl. The inset plot shows the raw ZF $-$ $\mu$SR spectrum taken at 3.1 K and the fitted curve using nine frequencies.

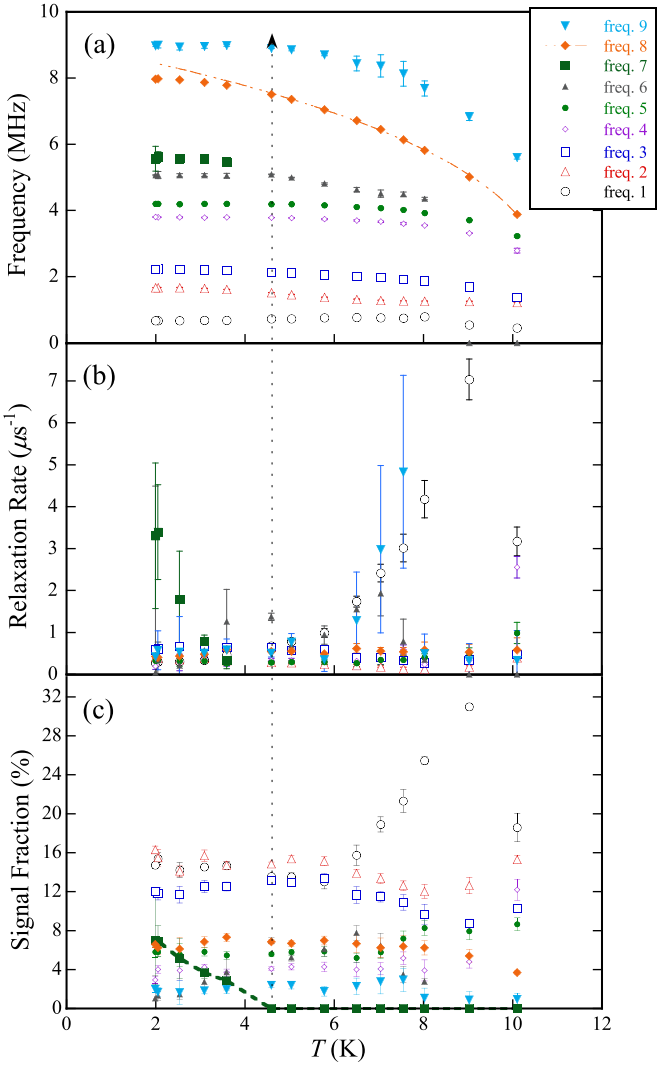


FIG. 7. Analyzed muon spin precession frequency, relaxation rate, and signal fraction for the nine signals observed in Cu(OH)Cl. The double dashed line in the frequency plot (a) is a fitted curve for a representative frequency obeying the formula $f = f_0(1 - \frac{T_N}{T})^\beta$ with $f_0 = 9.04(0.06)$ MHz, $T_N = 10.95(0.07)$ K, $\beta = 0.33(0.01)$.

nearby $Cl^-$ and was well fitted by the Kubo-Toyabe function $G_{KT}(t) = \frac{1}{3} + \frac{2}{3}(1 - (\gamma_\mu \sigma t)^2)e^{-\frac{1}{2}(\gamma_\mu \sigma t)^2}$, where $\sigma$ reflects the average nuclear dipolar field at the muon site.

In the magnetically ordered state of a polycrystalline sample, the longitudinal polarization function $P_Z(t)$ is expected to be the weighted sum of the longitudinal and transverse components: $P_Z(t) = \frac{1}{3}e^{-\lambda_Z t} + \frac{2}{3}e^{-\lambda_X t}\cos(\gamma_\mu \langle B_{loc}\rangle t)$. Therein, $\lambda_Z$ and $\lambda_X$, respectively, denote the spin-lattice and spin-spin relaxation rates, and $\langle B_{loc}\rangle$ stands for the mean value of the local field at the muon stopping site. If there are multiple muon stopping sites, the asymmetry would be accounted by the sum of damped oscillations. Below $T_N = 11$ K, all the muon spins precessed with multiple frequencies as shown in Fig. 6, directly demonstrating uniform local field in the sample, i.e., the long-range nature of its magnetic order. In this situation, the asymmetry was accounted for by damped oscillations with the damping due to spin-spin relaxation. The precession frequencies, the relaxation rates, and the signal fractions of the respective frequencies were exactly analyzed and shown in Fig. 7. Using one representative distinct signal double dashed in Fig. 7(a), the precession frequency change for $T > 5$ K can be well described by a power law $f = f_0(1 - \frac{T_N}{T})^\beta$, with $f_0 = 9.04(0.06)$ MHz, $T_N = 10.95(0.07)$ K, and $\beta = 0.33(0.01)$, implying that it can be used as an order parameter.

The most profound result from the $\mu$SR is the appearance of the additional frequency signal below $\sim$5 K [freq. 7 in Fig. 7(a)]. Actually, it should be viewed as a signal splitting from freq. 6, as the two frequencies slightly increased and decreased, respectively, from their average below $\sim$5 K. Looking back at Fig. 3(b), we can see that this signal appeared simultaneously with the dielectric constant jump and the microscopic anomaly in specific heat at $T^* \sim 5$ K. The signal fraction and relaxation rate of the freq. 7 signal below $T^*$ kept increasing until the lowest temperature. Muon site calculation suggested that the muons nearby the $Cl^-$ ions precessed with frequencies lower than $\sim$2 MHz, therefore the splitting of the freq. 6 signal into those of freq. 6 and freq. 7 below $T^* \sim 5$ K suggested one additional muon stopping site and a change in the local electric field nearby the $OH^-$. It is most probable that the sudden change in the local electric field resulted from a small structural change concerning the $OH^-$, i.e., the symmetry of the $P2_1/a$ crystal space group lowered

to produce asymmetric sites for the OH. Combined with the dielectric change, we conjectured a ferroelectric transition of spin origin below $T^* \sim 5$ K. It occurred in the vicinity of magnetic transition in this strongly magnetic-dielectric-coupled material, therefore it can be grouped into the multiferroic category.

## IV. SUMMARY

In summary, we have found magnetodielectric effect in hydroxyl salt CuOHCl, which is believed to be closely related to geometrical frustration on the triangular magnetic lattice. A microscopic probe of $\mu$SR suggested the possibility of a multiferroic transition at $T^* \sim 5$ K. The present triangular lattice antiferromagnet with a large interlayer spacing can be a prototypical model to study frustrated magnetic interactions and spin-related phenomena. There are only very few experimental realizations of the triangular lattice, in particular, multiferroic systems in slightly nonstoichiometric oxides, i.e., $CuFeO_2$ ($S = 5/2$), $CuCrO_2/AgCrO_2$ ($S = 3/2$), and $RbFe(MoO_4)_2$ ($S = 5/2$) [23]. The present system provides a structurally two-dimensional triangular lattice showing quantum spin-related properties, with coplanar spin configuration and perfect chemical stoichiometry.

## ACKNOWLEDGMENTS

This research is supported by a Grant-in-Aid for Scientific Research (B) (Grant No. 26289092) to X.G.Z. from the Japan Society for the Promotion of Science. The muon spin rotation/relaxation experiments at TRIUMF were performed under a user program (Experiment No. M1315). The neutron-diffraction experiment at the Materials and Life Science Experimental Facility of the J-PARC was performed under a user program (Proposal No. 2014A0183). A. Ohfuji and S. Yamaguchi prepared the sample for the powder neutron diffraction. The muon-site calculation is supported by the Large Scale Simulation Program No. 15/16-07 (FY2016) of High Energy Accelerator Research Organization (KEK). We are grateful to M. Hiraishi and to H. Lee and K. M. Kojima at Muon Science Laboratory, KEK, respectively, for discussion and muon-site simulation.

[1] For reviews see *Frustrated Spin Systems*, edited by H. T. Diep (World Scientific, Singapore, 2004); see also J. F. Sadoc and R. Mosseri, *Geometrical Frustration* (Cambridge University Press, Cambridge, England, 1999), reedited 2007.

[2] S. T. Bramwell and M. J. P. Gingras, Science **294**, 1495 (2001).

[3] L. Balents, Nature (London) **464**, 199 (2010).

[4] X. G. Zheng, H. Kubozono, K. Nishiyama, W. Higemoto, T. Kawae, A. Koda, and C. N. Xu, Phys. Rev. Lett. **95**, 057201 (2005); X. G. Zheng, T. Kawae, H. Yamada, K. Nishiyama, and C. N. Xu, *ibid.* **97**, 247204 (2006); X. G. Zheng, T. Kawae, Y. Kashitani, C. S. Li, N. Tateiwa, K. Takeda, H. Yamada, C. N. Xu, and Y. Ren, Phys. Rev. B **71**, 052409 (2005); X. G. Zheng, T. Mori, K. Nishiyama, W. Higemoto, H. Yamada, K. Nishikubo, and C. N. Xu, *ibid.* **71**, 174404 (2005); M. Hagihala, X. G. Zheng, T. Kawae, and T. J. Sato, *ibid.* **82**, 214424 (2010); M. Hagihara, X. G. Zheng, T. Toriyi, and T. Kawae, J. Phys.: Condens. Matter **19**, 145281 (2007); X. G. Zheng, M. Hagihala, K. Nishiyama, and T. Kawae, Physica B **404**, 677 (2009); M. Fujihala, M. Hagihala, X. G. Zheng, and T. Kawae, Phys. Rev. B **82**, 024425 (2010); M. Fujihala, X. G. Zheng, Y. Oohara, H. Morodomi, T. Kawae, A. Matsuo, and K. Kindo, *ibid.* **85**, 012402 (2012); S. E. Dissanayake, C. Chan, S. Ji, J. Lee, Y. Qiu, K. C. Rule, B. Lake, M. Green, M. Hagihala, X. G. Zheng, T. K. Ng, and S. H. Lee, *ibid.* **85**, 174435 (2012); M. Fujihala, X. G. Zheng, S. Lee, T. Kamiyama, A. Matsuo, K. Kindo, and T. Kawae, *ibid.* **96**, 144111 (2017).

[5] Y. Iitaka, S. Locchi, and H. R. Oswald, Helvetica Chimica Acta **44**, 2095 (1961).

[6] H. Effenberger, Mh. Chem. **115**, 725 (1984).

[7] Y. Cudennec, A. Riou, Y. Gerault, and A. Lecerf, J. Solid State Chem. **151**, 308 (2000).

[8] X. G. Zheng, M. Fujihala, S. Kitajima, M. Maki, K. Kato, M. Takata, and C. N. Xu, Phys. Rev. B **87**, 174102 (2013).

[9] S. Kitajima, M. Fujihara, X. G. Zheng, and T. Kawae, Exotic magnetism in a new quantum magnetic compound CuOHCl (in Japanese), in *Proceedings of the 117th Conference of the Kyushu Branch of Physics Society of Japan, 2011* (unpublished), http://www.phys.kyushu-u.ac.jp/kpsj/2011/program117-fin.pdf; S. Kitajima, M. Fujihara, X. G. Zheng, H. Morodomi, and T. Kawae, Magnetic transition in triangular-lattice compound CuOHCl, in *Proceedings of the Physical Society of Japan, 2013* (unpublished), Vol. 68, p. 876; S. Yamaguchi, A. Ohfuji, X. L. Xu, X. G. Zheng, Sanghyun Lee, Ping Miao, S. Torii, and T. Kamiyama, Neutron diffraction experiments and magnetic structure analysis of triangle lattice compound Cu(OD)Cl, in *Proceedings of the Physical Society of Japan, 2015* (unpublished), Vol. 70, p. 1045; S. Kitajima, M. Fujihala, and X. G. Zheng, *Investigation of the Magnetic States in New Quantum-Spin Systems of Spin Triangular Cu(OH)Cl and Spin-Tetrahedral $K_4Cu_4Cl_{10}O$*, KEK-MSL report, edited by R. Kadono, 2012 (unpublished), p. 71.

[10] R. Oishi, M. Yonemura, Y. Nishimaki, S. Toriia, Hoshikawa, T. Ishigaki, T. Morishima, K. Mori, and T. Kamiyama, Nucl. Instrum. Methods Phys. Res. A **600**, 94 (2009).

[11] F. Izumi and K. Momma, Solid State Phenom. **130**, 15 (2007).

[12] J. Rodriguez-Carvajal, Physica B (Amsterdam) **192**, 55 (1993).

[13] A. S. Wills, Physica B **276–278**, 680 (2000).

[14] L. F. Feiner, A. M. Oles, and J. Zaanen, Phys. Rev. Lett. **78**, 2799 (1997).

[15] F. Reynaud, D. Mertz, F. Celestini, J.-M. Debierre, A. M. Ghorayeb, P. Simon, A. Stepanov, J. Voiron, and C. Delmas, Phys. Rev. Lett. **86**, 3638 (2001).

[16] S. de Brion, M. D. Nunez-Regueiro, and G. Chouteau, Orbital and spin order in the triangular $S = 1/2$ layered compound $(Li, Na)NiO_2$, in *Frontiers in Magnetic Materials*, edited by A. V. Narlikar (Springer-Verlag, Berlin, 2005).

[17] A. J. W. Reitsma, L. F. Feiner, and A. M. Oles, New J. Phys. **7**, 121 (2005).

[18] J. B. Goodenough, D. G. Wickham, and W. J. Croft, J Phys. Chem. Solids **5**, 107 (1958).

[19] C. Darie, P. Bordet, S. de Brion, M. Holzapfel, O. Isnard, A. Lecchi, J. E. Lorenzo, and E. Suard, Eur. Phys. J. B **43**, 159 (2005).

[20] M. J. Lewis, B. D. Gaulin, L. Filion, C. Kallin, A. J. Berlinsky, H. A. Dabkowska, Y. Qiu, and J. R. D. Copley, Phys. Rev. B **72**, 014408 (2005).

[21] J. H. Brewer, S. R. Kreitzman, D. R. Noakes, E. J. Ansaldo, D. R. Harshman, and R. Keitel, Phys. Rev. B **33**, 7813 (1986).

[22] K. Nishiyama, S. W. Nishiyama, and W. Higemoto, Physica B **326**, 41 (2003).

[23] Y. Tokura, Rep. Prog. Phys. **77**, 076501 (2014).